Midinfrared second-harmonic generation in *p*-type InAs/GaAs self-assembled quantum dots

T. Brunhes, P. Boucaud,[a] and S. Sauvage
Institut d'Électronique Fondamentale, UMR CNRS 8622, Bât. 220, Université Paris-Sud, 91405 Orsay, France

F. Glotin, R. Prazeres, and J.-M. Ortega
CLIO/LURE, Bât. 209 D, Université Paris-Sud, 91405 Orsay, France

A. Lemaître and J.-M. Gérard
France Telecom CNET, 196 Av. H. Ravera, 92225 Bagneux, France

(Received 29 March 1999; accepted for publication 15 June 1999)

Resonant second-harmonic generation is reported in InAs/GaAs self-assembled quantum dots. Frequency doubling is observed between confined states in the valence band of the quantum dots. The second-order nonlinear susceptibility is maximum at 168 meV (7.4 μm wavelength) and is observed for an in-plane polarized excitation. A value of $\chi^{(2)}_{zxx}$ as large as 2×10^{-7} (m/V) is measured for one dot plane. A three-dimensional numerical calculation of the valence band states shows that the second-harmonic generation involves a resonant excitation between the h_{000} and h_{101} states and a state close to the continuum wetting layer states. © *1999 American Institute of Physics.* [S0003-6951(99)03932-7]

The linear and nonlinear response associated with optical transitions between confined states of self-assembled quantum dots has recently attracted wide interest. Midinfrared absorption between confined states in the conduction and in the valence band of InAs/GaAs self-assembled quantum dots has been reported.[1–3] This intraband absorption which occurs in the midinfrared spectral range is particularly appropriate for quantum dot infrared photodetection.[4] Apart from the linear optical response, self-assembled quantum dots are also expected to exhibit strong nonlinear effects. Indeed, it is well known that the nonlinear susceptibility can be substantially enhanced if resonance conditions can be achieved. This resonant enhancement applied to the case of intersubband transitions in quantum wells, has led to the observation of giant second- and third-order nonlinear susceptibilities in the midinfrared.[5–9] Recently, we have demonstrated that a record third-order nonlinear susceptibility can be obtained in *p*-type InAs/GaAs self-assembled quantum dots.[10] It has been shown that the enhancement of the nonlinear susceptibility, as compared to the bulk material, results from the values of the intraband dipole matrix elements (fraction of nanometer), the achievement of a double resonance condition and from the intrinsic narrow homogeneous linewidth of the intraband transitions. The question arises as to whether resonant midinfrared second-order nonlinearities can also be observed in self-assembled quantum dots. One prerequisite for second-order nonlinear processes is the lack of inversion symmetry. This condition is *a priori* satisfied for lens-shaped self-assembled quantum dots.

The quantum dot samples used for the experiments have been grown by molecular beam epitaxy. The *p*-type quantum dot sample consists of 40 InAs quantum dot layers separated by 35 nm GaAs barriers.[10] The quantum dot layers are inserted into the middle of a midinfrared waveguide grown on an n^+-doped GaAs substrate. The midinfrared waveguide consists of a 5.5 μm thick GaAs core grown above a 5 μm thick $Al_{0.9}Ga_{0.1}As$ cladding layer. The dot density is around $4\times10^{10}\,cm^{-2}$. The quantum dots are *p* doped with a beryllium δ-doping layer located 2 nm above each InAs layer. The nominal bidimensional carrier density is $6\times10^{10}\,cm^{-2}$. A reference sample with undoped quantum dots was separately used to calibrate the nonlinear susceptibility with the nonlinear susceptibility of bulk GaAs.

Nonlinear optical experiments were performed with the free-electron laser CLIO.[10] The second-harmonic signal was detected with a photovoltaic liquid-nitrogen-cooled InSb photodetector. The experiments were performed at room temperature. The free-electron laser pump beam was injected through the cleaved facet along the (110) direction of a 3 mm long sample. Two polarizers were set in front of the sample. The first polarizer was set at 45° while the second polarizer could be rotated providing a method to adjust the incoming polarization. A 6.7-μm-long wave-pass interference filter was set at the output of the free-electron laser beam, in order to remove any harmonic signal coming from the free-electron laser.

According to cross-section transmission electronic microscopy measurements, the quantum dots have a lens-shape geometry.[11] The energy level energies and the dipole matrix elements of the intraband transitions have been calculated by solving the three-dimensional Schrödinger equation for the present quantum dot geometry.[3] The energy levels h_{n_x,n_y,n_z} are indexed by reference to a parallelepipedal quantum dot with infinite potential barriers where confined states can be sorted according to the number of nodes n_x, n_y, n_z along the *x*, *y*, and *z* directions. In the midinfrared, the linear absorption spectrum of the waveguide sample, as reported in Ref. 10, is dominated by an absorption polarized along the growth axis of the quantum dots (*z* axis). This absorption, which is attributed to the $h_{000}-h_{001}$ transition is maximum at 110

[a]Present address: Department of Physics, Quantum Institute, University of California, Santa Barbara, CA 93106-9530; electronic mail: boucaud@qi.ucsb.edu

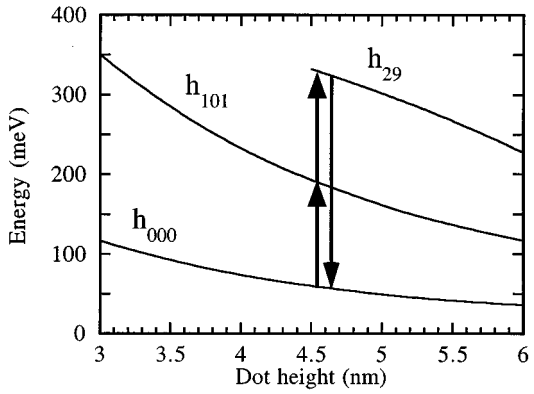

FIG. 1. Schematic diagram showing the quantum dot valence band states involved in the second-harmonic generation process. The energies of the confined states are given as a function of the quantum dot height. The ratio height diameter is 0.2. The arrows indicate the second-harmonic generation process. The wetting layer states are above 350 meV.

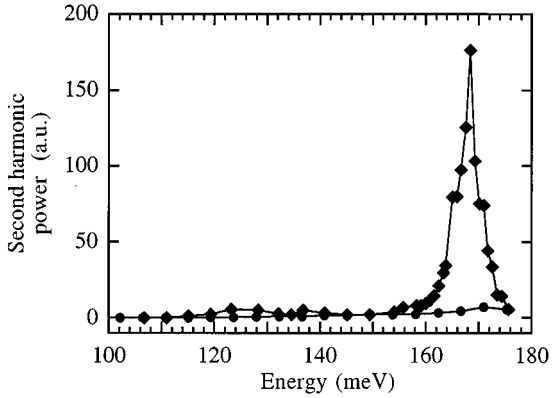

FIG. 2. Energy dependence of the second-harmonic power. The diamonds (dots) feature the power measured for the *p*-doped quantum dot (undoped) sample. The full curves are guides to the eyes. The pump excitation is in-plane polarized (TE polarization). The pump intensity is around 200 MW cm^{-2}.

meV with a full width at half maximum (FWHM) of 36 meV. A weak *z*-polarized absorption is also observed from the ground state to the continuum states with a maximum at 350 meV. A careful look at the absorption spectrum shows that an in-plane polarized absorption is also observed at 160 meV. This absorption is attributed to the $h_{000}-h_{101}$ transition. The experimental dipole length of this transition is 0.11 nm, in close agreement with the calculated 0.15 nm dipole length. A schematic diagram of the quantum dot valence band states is depicted in Fig. 1. The energies of some confined states are given as a function of the dot height. The intraband energies deduced from the calculation do not exactly match the experimental energies.[10] However, the dipole matrix elements are correctly predicted by the simulation. According to the three-dimensional calculation, the average quantum dot height, which corresponds to an $h_{000}-h_{001}$ absorption maximum at 110 meV, is 4.7 nm.[12] The transitions involved in the most efficient second-harmonic generation process are indicated on the graph. We note that an infrared excitation pump can be both in resonance with the $h_{000}-h_{101}$ intraband transitions and a transition from h_{101} to a state close to the wetting layer hybridized states. This situation corresponds to the double resonance condition.

Under high pump intensity regime, second-harmonic generation associated with the quantum dots was observed for pump wavelength below 11 μm. The collected signal was analyzed by a grating spectrometer providing an unambiguous signature of frequency doubling. We have separately checked that the second harmonic exhibits, as expected, a quadratic dependence with the incident pump power.[13] Frequency doubling could be obtained for a pump beam polarized either along the growth axis of the quantum dots (TM polarization) or in the layer plane (TE polarization). In the following, we will focus on the in-plane polarized second-harmonic generation which turns out to be the most efficient.

The spectral dependence of the second-harmonic power is reported in Fig. 2. The second-harmonic power is compared with the one measured with the undoped quantum dot reference sample, i.e., bulk GaAs, in the same experimental conditions. As seen, a strong enhancement of the frequency doubling is observed around 168 meV. The FWHM of this resonance is $\approx$5 meV. The resonance of the susceptibility is clearly not attributed to the achievement of phase matching for bulk second-harmonic generation at this particular wavelength since a similar effect would be observed for the undoped quantum dot reference sample.[14] A small resonance is also observed at 125 meV for the doped quantum dot sample. For the 168 meV resonance, the small broadening of the second-harmonic signal, as compared to the broadening of the absorption ($\approx$35 meV), is a clear signature of the resonant enhancement of the nonlinear susceptibility. It indicates that only a fraction of quantum dots satisfy the double resonance condition. The first transition involved in the second-harmonic generation process is the in-plane polarized $h_{000}-h_{101}$ transition. In order to observe resonant second-harmonic generation, a transition from the first excited state to a second excited state along with a transition from the ground state to the second excited state must have nonvanishing dipole matrix elements. The three-dimensional calculation of the energy levels shows that such a stringent condition is achieved for the quantum dots. A large number of states with an energy close to the wetting layer energy are confined in the dots. Among these states, the 29th confined state and to a lower extent the 28th, which is very close in energy satisfy both the condition on nonvanishing dipole and the resonance condition for second-harmonic generation.[15] The $h_{101}-h_{29}$ transition has an in-plane dipole matrix element of 0.21 nm. For the large dots, the $h_{000}-h_{29}$ transition has a theoretical *z*-dipole matrix element of 0.06 nm. The experimental absorption spectrum shows that a *z*-polarized transition is effectively allowed from the ground state to the states close to the continuum. Therefore, the nonlinear susceptibility experimentally measured is of the type $\chi^{(2)}_{zxx}$.

The second-harmonic power as a function of the polarizer angle is presented in Fig. 3. For this experiment, the pump energy was set at 168 meV. The second-harmonic powers of both doped quantum dot and undoped quantum dot reference samples are plotted in Fig. 3. The two curves do not exhibit a maximum at the same angles which indicates that the nonlinear susceptibility are not of the same origin. In the case of the reference sample, the second-harmonic generation stems from the bulk GaAs layer (non-

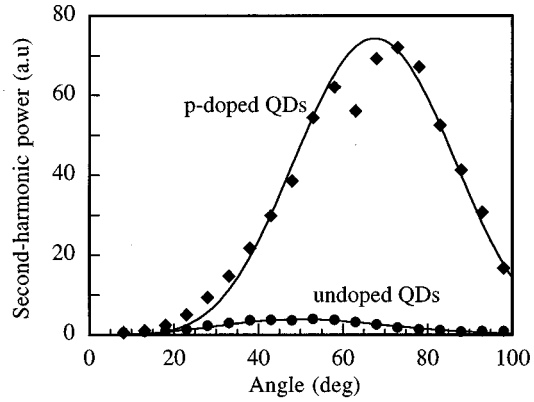

FIG. 3. Second-harmonic power (a.u.) as a function of the polarizer angle. Diamonds: *p*-doped quantum dot (QD) sample. Dots: undoped quantum dot reference sample. Full curves correspond to Eqs. (1) and (2).

vanishing $\chi^{(2)}_{zyx}$ component) which constitutes the core of the waveguide. The quantum dot nonlinear susceptibility is estimated in the same coordinates as the GaAs. Due to the quantum dot in-plane symmetry, both susceptibilities $\chi^{(2)}_{zxx}=\chi^{(2)}_{zyy}$ contribute to the harmonic signal. According to the experimental setup, the second-harmonic power is proportional to

$$P_{2\omega}\alpha|\chi^{(2)}_{zxx}|^2\sin^4\theta\cos^4(\theta-45)P^2_{\omega}, \tag{1}$$

$$P_{2\omega}\alpha|\chi^{(2)}_{zyx}|^2(1+3\cos^2\theta)\sin^2\theta\cos^4(\theta-45)P^2_{\omega}, \tag{2}$$

for the doped quantum dot and undoped quantum dot reference samples, respectively.

For the *p*-doped quantum dot sample, the contribution to frequency doubling of bulk and interference terms due to the GaAs substrate has been neglected. These curves are plotted as solid lines in Fig. 3. A satisfying agreement is found with the experimental results.

The experimental value of the nonlinear susceptibility can be deduced by two different methods. The susceptibility can be obtained from the amplitude of the collected second-harmonic power.[7] Using this method, the average susceptibility of the quantum dot sample is estimated as $\chi^{(2)}_{zxx}\approx 7.4\times10^{-10}$ m/V. However, this value depends on the exact collected power, on the exact intensity of the pump beam coupled in the waveguide, and on a phase matching assumption. A more accurate determination of the nonlinear susceptibility can be obtained by reference to the nonlinear susceptibility of bulk GaAs, as reported in Fig. 3. Starting from Eqs. (1) and (2) and assuming $\chi^{(2)}_{zyx}$ GaAs$\approx 1.9\times10^{-10}$ m/V,[16] one finds $\chi^{(2)}_{zxx}\approx 1.2\times10^{-9}$ m/V for the *p*-doped quantum dot sample. This value represents an average value of the nonlinear susceptibility over the 40 quantum dot layers embedded in the midinfrared waveguide. If we consider that the overlap of the quantum dot layers with the optical mode is 0.6%,[10] the nonlinear susceptibility for one dot layer plane is as large as 2×10^{-7} m/V. This value is three orders of magnitude larger than the nonlinear susceptibility of bulk GaAs. It is of the same order of magnitude that the $\chi^{(2)}_{zxx}$ susceptibilities associated with intersubband transitions in quantum wells.[6,7,17] In the latter case, the largest nonlinear susceptibilities have been observed for *n*-doped quantum wells, i.e., for an incident polarization along the *z* growth axis. In the present case, the resonant second-harmonic generation is observed for an in-plane polarized excitation.

The nonlinear susceptibility can be calculated theoretically by assuming that only the dot ground state is populated. For a three-level system close to the double resonance condition, the susceptibility at pulsation ω can be written as[18]

$$\chi^{(2)}_{zxx}=\frac{N_{3D}e^3}{\hbar^2\epsilon_0}\frac{x_{12}x_{23}z_{13}}{(\omega-\omega_{12}-i\gamma)(2\omega-\omega_{13}-i\gamma)}, \tag{3}$$

where x_{12},x_{23},z_{13} are the dipole matrix elements of the $h_{000}-h_{101}, h_{101}-h_{29}, h_{000}-h_{29}$ transitions, ω_{12} and ω_{13} the pulsations of the $h_{000}-h_{101}$ and $h_{000}-h_{29}$ transitions, and γ the half width at half maximum (HWHM) of the broadening. N_{3D} is the three-dimensional dot carrier density,[19] ϵ_0 the vacuum permittivity, and *e* the electronic charge. We assume that the intraband transitions are lifetime broadened and that the homogeneous broadening is similar to the broadening of the $h_{000}-h_{001}$ transition (200 μeV, HWHM).[10] The number of quantum dots which are optically excited by the free-electron laser is approximately given by the ratio between the laser linewidth and the absorption linewidth (3%). At double resonance, the theoretical value is therefore estimated as 4×10^{-8} m/V, if we take into account the weak contribution (30%) of the 28th level to the nonlinear susceptibility. The discrepancy between theoretical and experimental results is likely attributed to an underestimation of the dipole matrix elements and of the number of optically excited quantum dots and/or an overestimation of the homogeneous broadening.

[1] H. Drexler, D. Leonard, W. Hansen, J. P. Kotthaus, and P. M. Petroff, Phys. Rev. Lett. **73**, 2252 (1994).
[2] S. Sauvage, P. Boucaud, F. H. Julien, J. M. Gérard, and V. Thierry-Mieg, Appl. Phys. Lett. **71**, 2785 (1997).
[3] S. Sauvage, P. Boucaud, J.-M. Gérard, and V. Thierry-Mieg, Phys. Rev. B **58**, 10562 (1998).
[4] K. W. Berryman, S. A. Lyon, and M. Segev, Appl. Phys. Lett. **70**, 1861 (1997).
[5] M. M. Fejer, J. J. B. Yoo, R. L. Byer, A. Harwitt, and J. S. Harris, Jr., Phys. Rev. Lett. **62**, 1041 (1989).
[6] P. Boucaud, F. H. Julien, D. D. Yang, J. M. Lourtioz, E. Rosencher, P. Bois, and J. Nagle, Appl. Phys. Lett. **57**, 215 (1990).
[7] C. Sirtori, F. Capasso, D. L. Sivco, A. L. Hutchinson, and A. Y. Cho, Appl. Phys. Lett. **60**, 151 (1992).
[8] J. N. Heyman, K. Craig, B. Galdrikian, M. S. Sherwin, K. Campmann, P. F. Hopkins, S. Fafard, and A. C. Gossard, Phys. Rev. Lett. **72**, 2183 (1994).
[9] C. Sirtori, F. Capasso, D. L. Sivco, and A. Y. Cho, Phys. Rev. Lett. **68**, 1010 (1992).
[10] S. Sauvage, P. Boucaud, F. Glotin, R. Prazeres, J. M. Ortega, A. Lemaitre, J. M. Gérard, and V. Thierry-Mieg, Phys. Rev. B **59**, 9830 (1999).
[11] J. M. Gérard, J. Y. Marzin, G. Zimmermann, A. Ponchet, O. Cabrol, D. Barrier, B. Jusserand, and B. Sermage, Solid-State Electron. **40**, 807 (1996).
[12] The 4.7 nm effective height is greater than the quantum dot height.
[13] In Ref. 10 we mentioned that we did not observe frequency doubling around 12.5 μm wavelength, while third-harmonic generation turned out to be very efficient. In the present work, the pump is set at higher energy.
[14] D. B. Anderson and J. T. Boyd, Appl. Phys. Lett. **19**, 266 (1971).
[15] Only the heavy hole states are taken into account in the calculation.
[16] Z. H. Levine and D. C. Allan, Phys. Rev. Lett. **66**, 42 (1991).
[17] S. J. B. Yoo, M. M. Fejer, R. L. Byer, and J. S. Harris, Jr., Appl. Phys. Lett. **58**, 1724 (1991).
[18] Y. R. Shen, *The Principles of Nonlinear Optics* (Wiley, New York, 1984).
[19] N_{3D} corresponds to the bidimensional carrier density normalized by the 0.5 nm thickness of the InAs deposited layer.